Biomed Microdevices (2015) 17: 86
DOI 10.1007/s10544-015-9982-5

Novel scalable and monolithically integrated extracorporeal gas exchange device

Tina Rieper[1] · **Claas Müller**[1] · **Holger Reinecke**[1]

Published online: 7 August 2015

Abstract A novel extracorporeal gas exchange device (EGED) is developed, implemented and characterized. The aim hereby is to overcome drawbacks of state-of-the-art devices and of state-of-science approaches, like their labor intensive fabrication and their low volume density of the gas exchange area, respectively. As a consequence of the stacked setup of alternating layers of the blood compartment and the ventilation gas compartment, the developed EGED allows for double sided gas exchange. Furthermore, it enables an adaption to the diversity of medical requirements by scaling the amount of layers. The developed fabrication chain is used to fabricate leakage-free evaluation models and allows for a transition to automated fabrication. The EGED is completely fabricated in polydimethylsiloxane (PDMS) and features diffusion membranes, which are separating the compartments, with a mean thickness of 90 μm. With the evaluation models and oxygen as ventilation gas an oxygen transfer of 60 ml/l_{blood} (25 ml/(min m^2)) and a carbon dioxide transfer of 70 ml/l_{blood} (30 ml/(min m^2)) are achieved. The linear scalability of the concept as well as the functionality of the EGED with air as ventilation gas is shown.

Keywords Extracorporeal gas exchange · Silicone rubber processing · Gas transfer simulation · Large area bonding of microstructured PDMS sheets · Microstructured, thin PDMS sheets

✉ Claas Müller
claas.mueller@imtek.uni-freiburg.de

[1] Laboratory for Process Technology, Department of Microsystems Engineering - IMTEK, University of Freiburg, Georges-Koehler-Allee 103, 79110 Freiburg, Germany

1 Introduction

It is essential for life to maintain physiological oxygen and carbon dioxide partial pressures in the blood and hence in all body tissues. In health the necessary gas exchange with the environment is performed by the natural lung. In cases of a diseased or failing lung, it becomes vital to support the gas exchange between blood and environment. The conventional treatment of acute lung diseases or lung failure is mechanical ventilation, a method of mechanically supporting or replacing the spontaneous breathing of the lung. Disadvantage of the mechanical ventilation is that it bears the risk of ventilation associated lung injury, e.g., pulmonary barotrauma or volutrauma. Inflammatory processes in the lung tissue might decrease the gas permeability of the lung tissue and result in the necessity of an increased oxygen partial pressure in the ventilation gas. This non-physiological oxygen partial pressure promotes a pulmonary oxygen toxicity the lung tissue is exposed to. Therefore, the natural functionality of the lung is further reduced. (Oczenski 2012) An alternative is the usage of extracorporeal gas exchange devices (EGED) which support the gas exchange independent of the natural lung. Therefore, the lung is relieved and the chance of its recovery is enhanced. Such devices can be further used as a bridge to transplant. In the year 2014 the Extracorporeal Life Support Organization (ELSO) registered 5.037 cases of extracorporeal life support (ECLS). Since 1990 63.4 % of all registered ECLS cases were of respiratory nature, which are therefore accounting for approximately 3193 cases in 2014. (Bronzino 2000; ELSO 2015) EGEDs feature a blood compartment and a ventilation gas compartment separated by a diffusion membrane. The blood oxygenation and the removal of carbon dioxide take place by a diffusive gas exchange between the two compartments due to partial pressure gradients. State-of-the-art devices are mainly based on bundled or woven hollow

fibers which can either serve as blood compartment or as ventilation gas compartment. The hollow fibers are typically made of poly-4-methyl-1-pentene or microporous polypropylene. (Cove et al. 2012) One drawback of hollow fiber based devices is the dependency of their fabrication on labor intensive fabrication steps which are necessary to guarantee a leakage-free connection of the single hollow fibers and therefore the leakage-free separation of the two compartments. Besides, open porous hollow fibers imply the risk of plasma leakage through the fiber walls.

State-of-science approaches intend to increase the gas exchange efficiency of EGEDs by reduced diffusion lengths. This is achieved by thinner diffusion membranes or narrower blood paths in the blood compartment. In most approaches the blood compartment is realized as microchannels with a typical height in the range of 10 to 200 μm. The diffusion membranes are usually made of silicone rubber due to its high gas permeability. Diffusion membrane thicknesses used in these approaches range mainly between 10 μm and 150 μm. (Sillen et al. 2004; Kniazeva et al. 2011; Lee et al. 2008b; Potkay et al. 2011; Hoganson et al. 2010; Burgess et al. 2009; Wu et al. 2013) The drawbacks of state-of-science approaches are, besides others, the high risk of blockage of narrow blood paths in the blood compartment as well as a low integration density of the gas exchange area in the volume of the EGED. The device presented by Kniazeva et al., for example, consists of individual bilayer units of one layer of the blood and one of the ventilation gas compartment sandwiching a diffusion membrane. Each polydimethylsiloxane (PDMS) layer has a thickness of at least 1 mm. (Kniazeva et al. 2012) Therefore, the device only allows for single sided gas exchange and results in a comparably high necessary overall device height. Furthermore, for most other approaches no scalability and no concepts for highly integrated ready-to-use devices are presented so far.

The aim of the here presented work is to develop a concept of a microstructured EGED with highly and monolithically integrated blood paths. It allows for a simple scaling of the device to meet the diversity of requirements of patients of differing gender, weight and age. The conflicting requirements of such an EGED have been previously discussed in detail. (Rieper et al. 2013) Based on previously published work a fabrication chain is developed further which facilitates an automation of the whole fabrication process. (Rieper et al. 2012) Beyond, the gas exchange functionality of the developed EGED is characterized and its applicability is discussed.

1.1 Concept and gas exchange estimation

To outperform the low volume density of the gas exchange area in state-of-science approaches, the here presented approach of an EGED provides a high degree of integration and parallelization of layers of both compartments. Due to an alternate sequence of compartment layers and diffusion membranes, it allows for double sided gas exchange. To reduce the risk of clotting in the blood compartment, induced by turbulences or area of no flow, the blood flow is strictly guided within microchannels. This strict guiding and the resulting laminar flow causes a lack of mixing in the blood flow which results in a limited gas exchange due to a distinctive boundary layer. To overcome this drawback, the diffusion length within the blood has to be reduced. Both requirements are met if the blood flows through microchannels of low height (between 50 μm and 200 μm), in regard of a vertical gas exchange. The ventilation gas compartment is designed to allow a sufficient ventilation gas flow to prevent saturation of the ventilation gas with carbon dioxide or a significant depletion of oxygen. Furthermore, it is designed to have a minimal influence on the effective gas exchange area. For both reasons, it consists of a large open area supported by circular supporting structures. To gain the necessary degree of parallelization, layers of the two compartments are stacked alternately, separated by a thin polymer diffusion membrane as shown in Fig. 1. Due to its comparably high gas permeability P, PDMS is chosen as diffusion membrane material ($P_{O_2} = 9.2710^{(-13)}\mathrm{m}^2/(smmHg)$, $P_{CO_2} = 4.5610^{-12}\mathrm{m}^2/(\mathrm{smmHg})$). (Brandrup et al. 2004) To guarantee for a smooth transition and homogeneous distribution of the blood flow from the supply tubes to the single layers of the blood compartment, an in-plane approaching flow from one common manifold is realized.

For the layout of the diffusion membrane thickness and the blood compartment height, the resulting oxygen and carbon dioxide partial pressures in the blood compartment were mathematically estimated. Therefore, the mathematical model of Schultz et al., describing the oxygen and carbon dioxide diffusion through blood flowing in a microchannel, was adapted to the flow conditions of the EGED. (Schultz et al. 1977) As shear rates in the blood flowing through the blood compartment of more than 1000 s^{-1} are expected in the EGED, the flow behavior of the blood can be assumed as Newtonian resulting in a Hagen-Poiseuille flow profile. (Mazumdar 1992; Skalak et al. 1989; Eberhart et al. 1978; Caro et al. 1978) The governing equation, the mathematical model is based on (Eq. 1), results from Fick's first law and the mass balance equation for convective blood flow in x -direction and diffusive mass transfer in z -direction.

$$v_x(z)\ \frac{d\ c_i}{dz} = D_i \frac{d^2\ c_i}{dx^2} \tag{1}$$

$$c_i = c_{i,diss} + c_{i,hem} \tag{2}$$

Hereby, v_x describes the velocity profile for blood flow in x -direction (Hagen-Poiseuille flow profile), c_i is the gas concentration of species i (Eq. 2) considering physically dissolved gas molecules ($c_{i,diss}$) given by Henry's law as well as those chemically bound to hemoglobin ($c_{i,hem}$) given by the gas

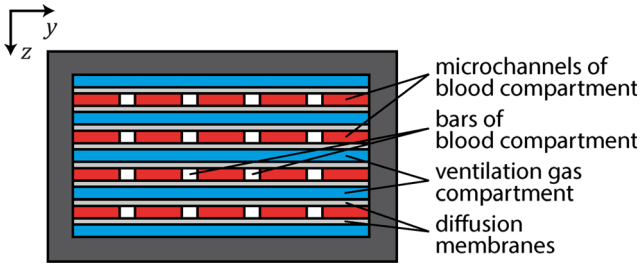

Fig. 1 Conceptual cross section through the EGED. Blood is guided through the blood compartment in microchannels. The ventilation gas compartment is supported by circular posts (not shown)

dissociation curves. A mathematical model of the oxygen dissociation curve is given by Margaria (1963). The carbon dioxide dissociation curve is mathematically described by Harris et al. (1970).

The gas exchange and therefore the resulting partial pressures are assumed to be independent of the y -direction, i.e., along the blood compartment width, allowing for a two dimensional mathematical model. Furthermore, the oxygen and carbon dioxide diffusion are regarded separately and as independent.

The governing equation, a partial differential equation, is approximated by the finite difference method. The approximated governing equation is then solved by the iterative Newton's method. (Kelley 2003) The partial pressures resulting from the diffusive gas exchange of oxygen and carbon dioxide were estimated in dependency of the blood compartment height (10 to 200 μm), the diffusion membrane thickness (10 to 150 μm) and the mean blood flow velocity (10 to 30 mm/s) with this method. Exemplary simulation results of the gas partial pressures are depicted in Fig. 2 for a mean blood flow velocity of 20 mm/s for oxygen (*top left*) and for carbon dioxide (*top right*). The simulation results for the oxygen partial pressure were further transferred to the oxygen saturation in the blood using the mathematical model of the oxygen dissociation curve given by Margaria et al. (1963). The oxygen saturation is shown in Fig. 2 (*bottom left*).

The simulation results illustrate the decrease of the resulting gas exchange with increasing diffusion membrane thickness and increasing blood compartment height which results in a lower oxygen partial pressure and a higher carbon dioxide partial pressure for a given blood compartment length. Thereby, the influence of the blood compartment height exceeds the influence of the diffusion membrane thickness. Comparison of the investigated blood flow velocities (not depicted) further shows that the achieved oxygen partial pressure decreases and the carbon dioxide partial pressure increases with increasing blood flow velocity. As a result of the higher blood volume flow through the EGED with increased blood flow velocity, the gas exchange per time, however, might be constant or even increase. This fact is not considered for the design derivation. To guarantee for a sufficient carbon dioxide removal a carbon dioxide partial pressure of 25 mmHg is aimed at the blood compartment outlet. To ensure a sufficient oxygenation of the blood by the EGED the simulated oxygen outlet partial pressure has to be maximized (760 mmHg). The occurring pressure drop per blood compartment length and the maximum shear rate in blood were calculated for all investigated blood compartment length and blood flow velocity combinations reaching the aimed carbon dioxide partial pressure within a blood compartment length of 250 mm. For the calculation an approximation of the blood viscosity, describing its dependency on the hematocrit (44 %) and the temperature (310 K) was used. (Mazumdar 1992; Baskurt 2007). The results are summarized in Fig. 3. A complete oxygen saturation of the blood is gained by the simulation for all investigated geometry combinations. The aimed carbon dioxide partial pressure is reached by the simulation, besides other combinations, for a blood compartment height of 100 μm, a diffusion membrane thickness of 100 μm and a mean blood flow velocity of 20 mm/s within a blood compartment length of 150 mm. These values are considered for the EGED as the diffusion membrane thickness seems to be feasible for manual fabrication of defect free diffusion membranes. Furthermore, these values are a trade-off between the pressure drop, the shear rate and the blood volume flow. The investigation of the theoretical Hagen-Poiseuille flow profile for a blood flow velocity of 20 mm/s and a blood compartment height of 100 μm shows maximal occurring shear rates of more than 1200 s^{-1}. Therefore, the assumption of Newtonian flow behavior seems justified.

The microchannels of the blood compartment have a width of 1 mm and are separated by 500 μm wide bars. In one layer of the blood compartment 40 microchannels are arranged in parallel. The circular supporting structures of the ventilation gas compartment have a diameter of 500 μm, a height of 200 μm and are arranged in a way that they will be positioned above the microchannel bars of the blood compartment in the stacked device. By this arrangement a minimal reduction of the gas exchange area by the supporting structures is realized. To shorten the ventilation gas compartment length, and therefore the pressure drop within the ventilation gas flow, two ventilation gas compartments are arranged in parallel, perpendicular to the blood compartment. A schematic of the compartment arrangement is shown in Fig. 4.

The fabrication strategy for the EGED has to facilitate the possibility of arranging highly parallelized layers of the two different compartments with 100 μm thick diffusion membranes in between. A monolithic fabrication of the device is not possible due to the complex arrangement of supporting structures necessary within the compartments and the low aspect ratios of the compartments. Therefore, a fabrication of the device by layers is considered. Hereby, sheets of the PDMS diffusion membrane facilitating the supporting structures of the later underlying compartment are stacked and

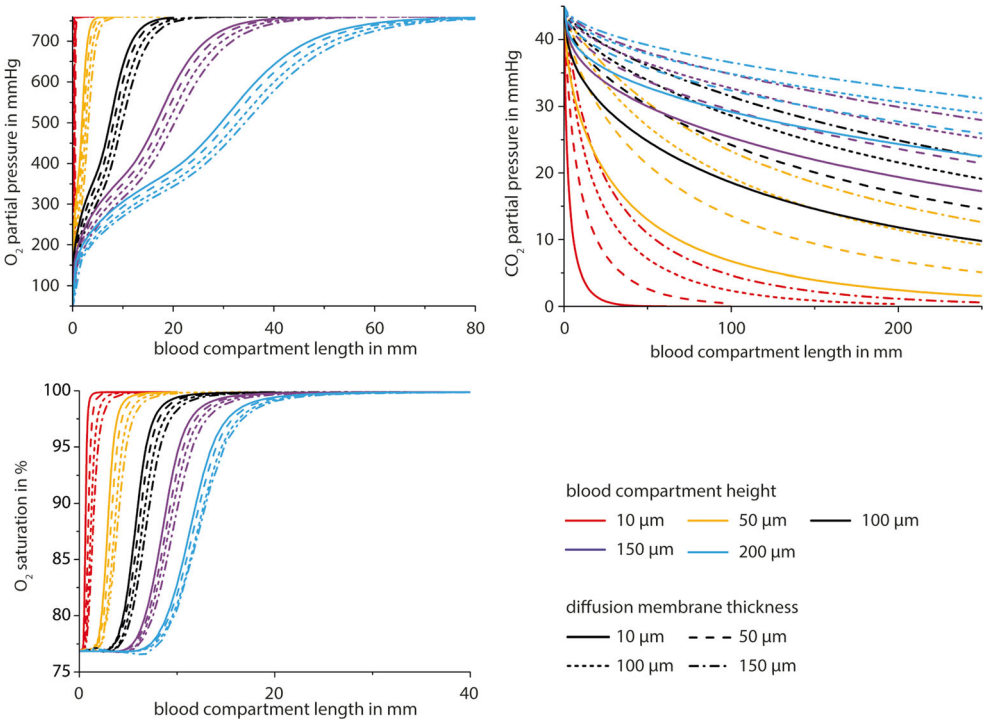

Fig. 2 Simulation results of the oxygen (*top left*) and the carbon dioxide (*top right*) partial pressures resulting from the diffusive gas exchange while considering a mean blood flow velocity of 20 mm/s. A two dimensional mathematical model of the partial pressures was used, as the gas partial pressures are assumed to be constant along the blood compartment width. Oxygen saturation (*bottom left*) in the blood calculated from the simulation result of the oxygen partial pressure via the mathematical model of the oxygen dissociation curve given by Margaria et al. (1963)

surface bonded to each other to realize the device. The integration of the supporting structures to the diffusion membrane and fabricating them consequently also in PDMS avoids the challenge of bonding PDMS to other materials and results in a monolithically integrated device. The arrangement of the inlet and outlet structures of the three distinctive compartments allows independent fluidic connection of the compartments. The inlet and outlet regions are designed to distribute the fluids homogenously within a small length and are further supported by pillars. The PDMS sheets, i.e., the diffusion membranes featuring the supporting structures of either the blood compartment or the ventilation gas compartments, are fabricated by casting structured brass tools. By an alternating stacking of PDMS sheets with the supporting structures of either the blood compartment or the ventilation gas compartments, the layers of the compartments are highly parallelized and allow for a double sided gas exchange. The stack of PDMS sheets is reinforced and protected against impact from the environment by thicker PDMS housing plates on the top and the bottom of the stack. Fluidic connectors fabricated in PDMS are subsequently fixed to the inlet and outlet regions of the three compartments as common manifolds for all corresponding layers.

2 Monolithically integrated fabrication

The fabrication process of the EGED has to ensure a leakage-free setup to guarantee a safe application of the EGED in an extracorporeal blood circuit. Furthermore, the fabrication should allow an easy transition to an automated fabrication. For a monolithically integrated fabrication of the EGED, the PDMS sheets are bonded to each other by curing a thin PDMS interlayer. By this method a reliable bonding can be realized

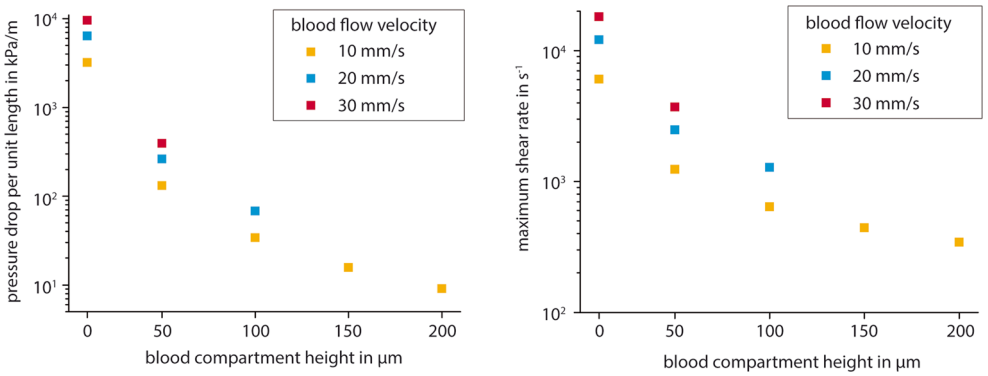

Fig. 3 Theoretically estimated pressure drop per length (*left*) and maximum shear rate (*right*) of blood compartment length and blood flow velocity combinations accomplishing a simulated carbon dioxide partial pressure of 25 mmHg within a blood compartment length of 250 mm. For a better visibility the y-axes are logarithmic

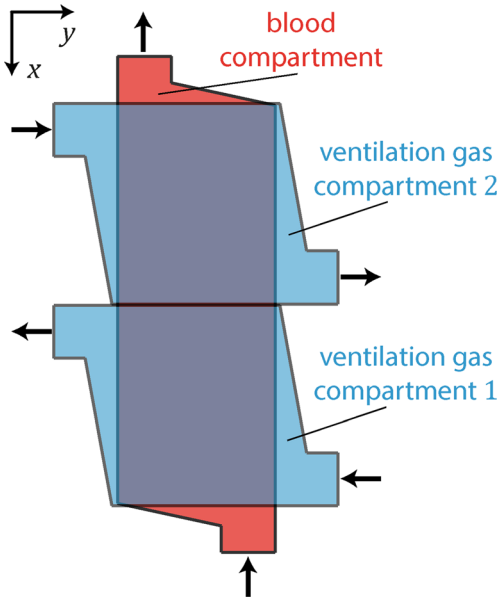

Fig. 4 Schematic arrangement of the compartments in the EGED. The gas exchange area of the blood compartment is covered by two parallel ventilation gas compartments which are separated by a 500 μm wide bar. The arrows give the flow directions at the inlet and outlet regions of each compartment. The flows within the compartments are directed to guarantee as homogeneous and as high partial pressure differences as possible between the blood compartment and the ventilation gas compartments

even on large surfaces as for the EGED (> 160 cm^2). The fabrication process of the EGED, shown in Fig. 5, can be divided into four major steps: i) the fabrication of the PDMS sheets, ii) the assembly of the sheets, iii) the fabrication of the fluidic connectors and iv) the fluidic connection of the stack to the macro periphery. Afterwards the device is ready to use and does not require any further assembly or post processing steps.

For the fabrication of each PDMS sheet 15 g of PDMS (Elastosil® RT601, Wacker Chemie AG, München, Germany) are prepared according to the datasheet and evacuated in a desiccator. The chosen PDMS was tested to be non-hemolytic according to ISO 10993–1 for medical devices in a comparative study. The casting tool consists of two brass plates, one facilitating the negative structures of the compartment (tool plate) and an unstructured one (cover plate), a steel frame (thickness of either 200 μm for the blood compartment or 300 μm for the ventilation gas compartments) and a polyimide (PI) foil. The steel frames are fabricated by wire electrical discharge machining of precision steel sheets (1.4310) due to the narrow tolerated thickness. A comparably rough machining strategy is used, to achieve a high arithmetic mean roughness of R_a=3 μm. (Charmilles Technologies 1997) The cutting faces of high arithmetic mean roughness facilitate a mechanical interlocking between steel frame and PDMS sheet. The steel frame is mounted on the tool plate with alignment pins. The PDMS is poured onto the tool plate within the steel frame and covered by the PI foil. The tool is closed with the cover plate. A pressure of 320 kPa is applied on the casting tool in a hot embossing machine (MB 25200VC, Schmidt Maschinentechnik, Bretten, Germany) while the temperature is increased to 70 °C. After 15 min the casting tool is cooled down again, the pressure is released and the casting tool can be opened. The cured PDMS sheet is demolded within the steel frame. Most obviously the steel frames define the thickness of the PDMS sheets and therefore the diffusion membrane thickness. Furthermore, the steel frames define the outer geometry of the PDMS sheets and allow their non-destructive handling including their demolding, their cleaning, the application of the PDMS interlayer on the sheets and the precise alignment of the sheets to each other. A thin PDMS interlayer is applied onto the elevated structures of the structured side of the PDMS sheets via a transfer roll. Therefore, 0.3 ml of uncured PDMS is spread on a glass work bench on an area of 600 cm^2 via the transfer roll. After the complete wetting of the transfer roll with uncured PDMS, the interlayer is applied on the structured PDMS sheet by rolling the transfer roll over the structured side of the PDMS sheet several times in each direction. The PDMS sheet is then placed structured side down on a 1.5 mm thick unstructured PDMS housing plate. The stacking of the PDMS sheets and housing plates is executed on a polycarbonate base plate facilitating alignment pins. In combination with the guiding holes of the steel frames the alignment pins allow for accurate alignment of the PDMS sheets to each other. The first PDMS sheet processed this way is a PDMS sheet with the supporting structures of the ventilation gas compartments. Each subsequent PDMS sheet with applied PDMS interlayer is then placed face down on the already stacked sheets. Subsequently, the steel frames are removed. The stack is finished by a second unstructured 1.5 mm thick PDMS housing plate. The inlet and outlet regions of each compartment are opened by cutting along the edge of the stack with a scalpel. The PDMS interlayers are cured in a furnace at 130 °C. The fluidic connectors are made of a platinum catalyzed silicone tube which is embedded in a PDMS mold. The commercially available silicone tube has an inner diameter of 6 mm and can be connected, for example, to a pumping tube via standard barb connectors. The fluidic connectors are assembled to the inlet and outlet regions of the stack with uncured PDMS which is subsequently cured in a furnace at 70 °C.

With this fabrication chain leakage-free evaluation models of the EGED were fabricated with up to 21 layers (10 layers of the blood compartment and 11 layers of the ventilation gas compartments). Due to fabrication tolerances regarding the height of the negative compartment structures on the used tool plates of the casting tools, a mean diffusion membrane thickness of 90 μm instead of the aimed 100 μm was realized. Therefore, an increased gas exchange is expected. For the comparison with the experimental results the gas exchange simulation is adapted to the actual mean diffusion membrane

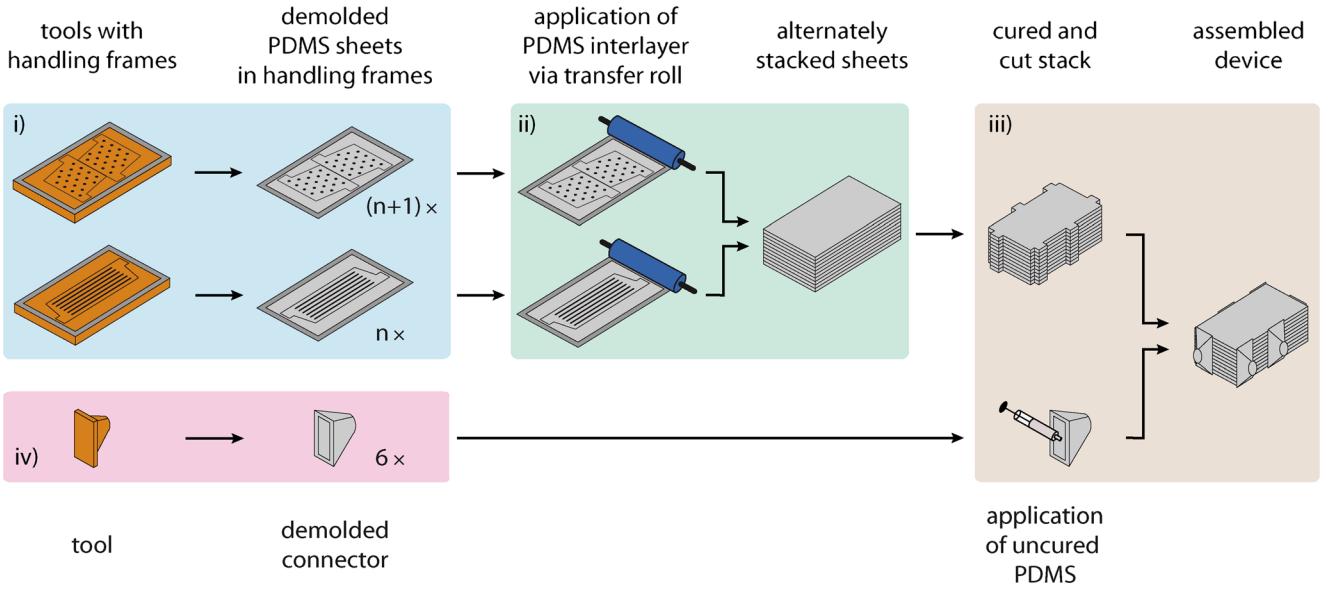

Fig. 5 Schematic overview of the fabrication process of the EGED divided into four major steps: i) the fabrication of the PDMS sheets, ii) the assembly of the sheets, iii) the fabrication of the fluidic connectors and iv) the connection of the stack to the macro periphery

thickness. A fabricated evaluation model is shown in Fig. 6. A limitation of the number of stacked layers was not observed.

The cured PDMS interlayers have a thickness of approximately 6 µm and do not affect the compartment cross sections (see Fig. 7). A slight misalignment of maximal 200 µm is observed between the layers of the compartments. This most probably results from the manual stacking process. The bond strength between the layers was verified with testing models of reduced size and complexity to be 1.4 N/mm^2.

3 Gas exchange characterization

The gas exchange of the EGED is characterized with heparinized porcine blood as test medium. The porcine blood is collected from a slaughter house and used for the characterization within 6 h. The blood is heparinized with 4500 IU per liter blood. The blood is filtered with a 40 µm filter to prevent clogging of the blood compartment by debris or thrombi in the blood. Debris might be introduced into the blood during the slaughtering. Thrombi might also occur during the storage of the blood. The blood is kept in a reservoir at 37 °C and continuously stirred to prevent cell sedimentation. The blood is conditioned according to ISO 7199:2009. Important conditioning parameter and their values are summarized in Table 1. All parameters are monitored during the experiments. For each evaluation model of the EGED and each experiment day a fresh batch of blood is used. The characterization is performed with evaluation models of the EGED with 7 layers, i.e., 3 layers of the blood compartment and 4 layers of the ventilation gas compartments. As ventilation gas either pure oxygen or air is used. Preliminary to the experiments the evaluation model of the EGED is filled with water of reduced surface tension (spiked with isopropyl), to improve the wetting of the microchannels and therefore to reduce the risk of trapped air bubbles. Subsequently the evaluation model is rinsed by pumping physiological saline solution through it. The conditioned porcine blood is pumped through the evaluation model by a peristaltic pump (LA-900, Landgraf Laborsysteme HLL GmbH, Langenhagen, Germany) with which the blood flow is adjusted to 21 mm/s (15 ml/min). The blood gases are analyzed with a commercial blood gas analyzer (ABL 715, Radiometer GmbH, Willich, Germany). For each parameter set three subsequent analyses are evaluated.

The evaluation models show outstanding blood flow characteristics within the blood compartment of the EGED. All layers of the blood compartment are filled homogeneously with blood. No significant differences in the blood flow of the microchannels and layers of the blood compartment are observed during the experiments which could be related to their differing positions in relation to the manifolds. Even after blood flowing through the EGED for more than 3 hours, no

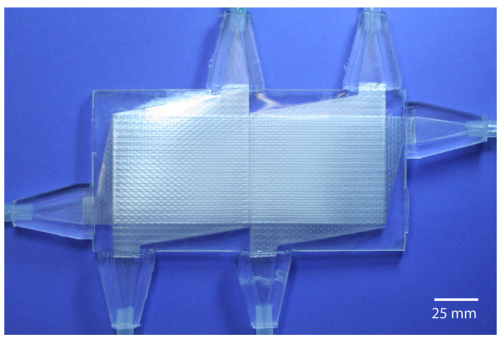

Fig. 6 Evaluation model of the EGED with 21 layers

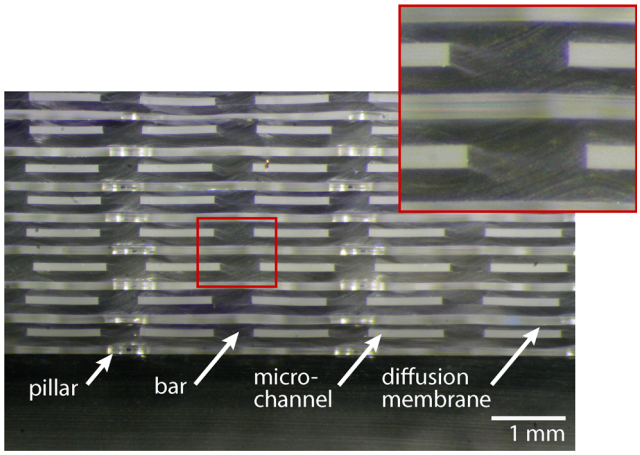

Fig. 7 Cross section and detail view of an evaluation model of the EGED with 100 μm ventilation gas compartment height. Adapted from Rieper et al. (2012)

thrombi or clogging of the microchannels are observed. For a blood flow velocity of 21 mm/s (15 ml/min) a maximum pressure drop of 10.7 kPa occurs. Within the duration of an experiment no alteration of the pressure drop is observed. Within the microchannels of the blood compartment (neglecting the inlet and outlet regions of the layers of the blood compartment as well as the manifolds) a pressure drop of 9.1 kPa is expected theoretically for the actual microchannels dimensions. An additional pressure drop of maximal 1.6 kPa due to the inlet and outlet regions of the layers of the blood compartment and the manifolds seems reasonable. No distinctive cell-free layer at the microchannel walls, due to axial migration of RBCs, is observed in a detailed investigation for whole blood flowing through microchannels equal to those of the EGED. (Rieper et al. 2014) The existence of such a cell-free layer would negatively influence the gas exchange efficiency as a result of increased diffusion lengths.

With the evaluation models and oxygen as ventilation gas an oxygen transfer of 60 ml/l_{blood} and a carbon dioxide transfer of 70 ml/l_{blood} are achieved. Due to the blood flow rate of 5 ml/min and a gas exchange area of 0.012 m^2, both per layer of the blood compartment, these gas exchange values correspond to 25 ml/(min m^2) for oxygen and 30 ml/(min m^2) for carbon dioxide. Gas transfer results for two evaluation models (*A* and *B*) identically constructed and a blood flow velocity of 21 mm/s (15 ml/min) are shown in Fig. 8 for oxygen (*left*) and for carbon dioxide (*right*). Furthermore, the gas exchange is estimated by the above presented mathematical model for the conditions present in the experiments and is given in Fig. 8 for comparison. The gas transfer showed no distinct dependency on the ventilation gas flow. In the outflowing blood a superb oxygen saturation ranging from 98.5 to 99.4 % and a carbon dioxide partial pressures ranging from 31 to 34 mmHg are achieved.

Table 1 Blood conditioning parameter according to ISO 7199:2009 "Cardiovascular implants and artificial organs—Blood-gas exchangers"

Parameter	Unit	Value	Tolerance
Oxygen saturation	%	65	± 5
Carbon dioxide partial pressure	mmHg	45	± 5
Hemoglobin content	g/dl	12	± 1
Base excess	mmol/l	0	± 5

For air as ventilation gas an oxygen and a carbon dioxide transfer of 32 ml/l_{blood} (13 ml/(min m^2)) and 67 ml/l_{blood} (28 ml/(min m^2)) are achieved, respectively. As expected the oxygen transfer decreases due to the reduced oxygen partial pressure (21 %) of the ventilation gas while the carbon dioxide transfer is only minimally influenced.

The scalability of the EGED is shown with evaluation models of the EGED consisting of 7 and 21 layers (corresponding to 3 and 10 layers of the blood compartment, respectively), oxygen as ventilation gas, water as test medium and a flow velocity of 21 mm/s (corresponding to a constant flow rate of 5 ml/min per layer of the blood compartment). Water is used as test medium due to the higher consistency of its properties and therefore better comparability of the experimental results in comparison to blood as test medium. No influence on the gas exchange characteristics per layer of the blood compartment is observed due to the scaling from 3 to 10 layers of the blood compartment (oxygen exchange of 25 ml/(min m^2) and carbon dioxide exchange of 30 ml/(min m^2)). The overall gas exchange of the evaluation model consisting of 21 layers increases according to the increased amount of layers of the blood compartment.

4 Discussion

The oxygen transfer of the two identically characterized evaluation models with blood as test medium differs by up to 3.5 ml/l_{blood} (5.8 %). This difference might result mainly from tolerances in the manual fabrication of the evaluation models, like variations in the diffusion membrane thickness or misalignments in the stacking of the PDMS sheets. Furthermore, the distinctive blood batch might slightly vary in their properties regarding their ability to be oxygenated and the carbon dioxide removal. The characterization results exceed the value determined by simulation by approximately 10 %. The reason might be imprecisions in the assumptions made for the simulation, like the assumed oxygen dissociation model which describes the relationship of the chemically bound oxygen to the oxygen partial pressure.

The carbon dioxide transfer of the two identically characterized evaluation models with blood as test medium differs by up to 1.3 ml/l_{blood} (1.8 %) which is within the range of deviation observed for each evaluation model.

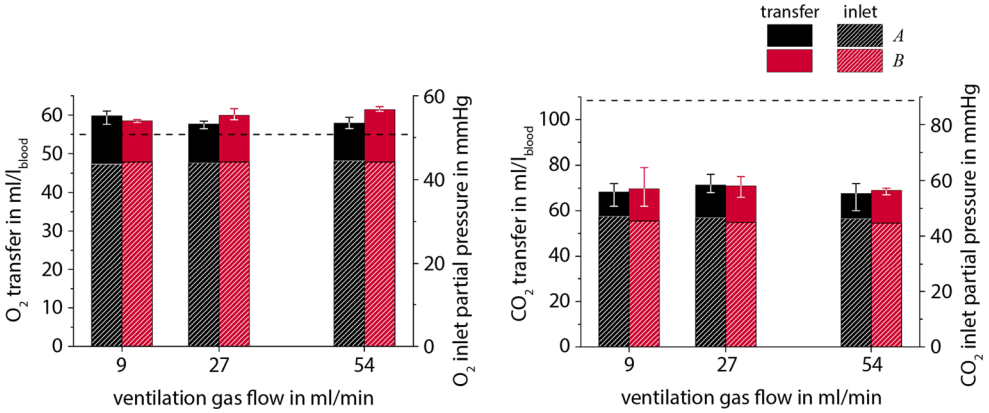

Fig. 8 Oxygen transfer (*left*) and carbon dioxide transfer (*right*) of 2 evaluation models (*A* and *B*) of 7 layers for oxygen as ventilation gas and a blood flow velocity of 21 mm/s (corresponding to a blood flow rate of 15 ml/min). The height of the bars gives the average of three subsequent analysis and the error bars give their range. The hatched areas give the oxygen and carbon dioxide inlet partial pressure of the blood for the experiment. For comparison the simulated values are given as dashed line

Within the experiments the carbon dioxide transfer achieves only 65 % of the value determined by simulation for the given conditions like partial pressures in the ventilation gas, diffusion membrane thickness and microchannel dimensions. This difference cannot be explained completely by imprecisions of the carbon dioxide dissociation model the simulation is based on. More reasonable is an imprecision of the simulation as the oxygen and carbon dioxide transfer are considered separately and as independent of each other. Due to the large excess of oxygen present in the EGED, oxygen diffusion is predominant. Therefore, the residual free volume within the diffusion membrane available for the carbon dioxide diffusion is reduced, and hence, the carbon dioxide diffusion is decreased. This fact is not considered by the simulation leading to an overestimation of the carbon dioxide transfer. This might be one reason of the overestimation of the carbon dioxide transfer by the simulation. That the carbon dioxide transfer is overestimated by the same amount for air as ventilation gas might still be caused by the large oxygen excess (160 mmHg oxygen in the ventilation gas vs. a maximum of 45 mmHg carbon dioxide in the blood). Furthermore, the pressure is higher in the blood compartment than in the ventilation gas compartment. This fact may result in a bowing of the diffusion membrane and therefore in an increased blood compartment height. As seen in Fig. 2 an increase of the blood compartment height does not influence the oxygen transfer, as it is already saturated for much shorter blood compartment lengths, but strongly influences the carbon dioxide transfer. Therefore, only an influence on the carbon dioxide transfer is expected by increasing blood compartment heights as seen in the experiments.

5 Conclusions

To overcome the drawbacks of state-of-the-art EGEDs, like their labor intensive fabrication, and of state-of-science approaches, like their low integration density of the gas exchange area in the volume of the EGED, a novel concept for a scalable and monolithically integrated EGED was developed and implemented. The developed EGED is constructed as a stack of alternate layers of the blood compartment and the ventilation gas compartments. Each layer of the EGED consists of a PDMS sheet featuring one diffusion membrane and the supporting structures of the underlying compartment. This stacked setup allows for a high degree of integration and parallelization of the compartment layers resulting in a high volume density of the gas exchange area, and furthermore, in a double sided gas exchange for each compartment layer. To enable the non-destructive handling, cleaning, further processing and positioning of the thin PDMS sheets, the PDMS sheets are manufactured within steel frames. The bonding between the single sheets is performed by curing a PDMS interlayer.

By the developed fabrication method monolithically integrated, ready-to-use evaluation models of the EGED are fabricated in contrast to many state-of-science works presented in literature. (Lee et al. 2008a; Burgess et al. 2009; Potkay et al. 2011; Wu et al. 2013) Other works presented in literature are outperformed by means of the volume density of the gas exchange area and therefore the degree of integration. (Kniazeva et al. 2011; Kniazeva et al. 2012; Rochow et al. 2014) Leakage-free evaluation models of the EGED with a mean diffusion membrane thickness of 90 µm were fabricated consisting of 7 and 21 layers. The blood compartment of an evaluation model consisting of 21 layers incorporates 400 parallel microchannels. A restriction on the amount of stacked layers is not observed during the fabrication. A diffusion membrane thickness of initially 100 µm was chosen to ensure the feasibility of a manual fabrication of the evaluation models. However, the study showed that even the manual fabrication of diffusion membrane thicknesses down to 50 µm is possible.

The fabrication of the EGED has the potential to be highly automated, in contrast to hollow fiber based state-of-the-art devices and state-of-science approaches basing on microstructured compartments. The fabrication of the PDMS sheets as well as the connectors could be performed by injection molding or in a highly parallelized molding process. The idea of the in-mold steel frames can be transferred directly to both fabrication techniques. The PDMS interlayer can be applied in a standard lamination process. The assembly of the device as an alternate stacking of the PDMS sheets could be realized in a pick and place technique. With this approach an accurate alignment of the PDMS sheets can be realized utilizing alignment structures in the steel frames. Disadvantage is the necessity of a complex fabrication line. Alternatively, the stacking process could be integrated in the lamination process. However, the accurate alignment of the PDMS sheets to each other would be more challenging and necessitate the development of a specialized lamination process.

The developed fabrication chain is not only restricted to the fabrication of EGEDs but may be advantageous whenever manifold, accurate stacking and full facial bonding of microstructured, thin, large-scale PDMS substrates is required.

The gas transfer per blood volume achieved with the developed EGED is comparable with state-of-the-art hollow fiber based devices (oxygen transfer ranging between 50 ml/l_{bood} and 88 ml/l_{bood}; carbon dioxide transfer ranging between 44 and 115 ml/l_{bood}). In comparison to state-of-the-art hollow fiber based devices the blood volume flow of 5 ml/min per layer of the blood compartment is significantly lower. Therefore, the gas transfer per minute and diffusion membrane area is by far lower than for state-of-the-art hollow fiber based devices. This fact restricts the advantage of the developed EGED to applications of low blood volume flow as for example applications with neonates as discussed below. Furthermore, the lower blood volume flow results in the necessity of about twice the priming volume of state-of-the-art multilayer microfluidic devices (ranging between 175 and 275 ml) due to the necessary parallelization. (Novalung 2009; Medos Medizintechnik 2007; Novalung 2009; Medtronic Inc 2011; Maquet Cardiopulmonary 2012) Promising advantage of the EGED over hollow fiber based state-of-the-art devices is the possibility of a complete automation of the fabrication. Furthermore, the gas exchange is comparable with promising state-of science multi-layer microfluidic approaches. Wu et al. (2013) presents a by far higher carbon dioxide transfer of 92 ml/(min m^2) but an oxygen transfer of only 15 ml/(min m^2) achieved with microporous PDMS diffusion membranes of 15 μm thickness, a blood compartment height of 80 μm and air as ventilation gas. The work of Kniazeva et al. (2012) achieves a by far higher oxygen transfer of 223 ml/(min m^2) with 117 μm thick PDMS diffusion membranes, a blood compartment height of 50 μm and oxygen as ventilation gas. However, Kniazeva et al. (2012) does not state any information about the carbon dioxide transfer. With single layer devices even higher gas exchange has been achieved (Lee et al. 2008a, b; Potkay et al. 2011). Anyway, most of the multi-layer or single layer approaches have an increased risk of blockage of narrow blood paths in the blood compartment as well as a low integration density of the gas exchange area in the volume of the EGED in common.

In rest a healthy adult approximately consumes 250 ml/min of oxygen and produces 200 ml/min of carbon dioxide. (Bungay et al. 1986) To cover the necessary gas exchange by the here developed EGED in total, an EGED consisting of 833 layers of the blood compartment would be necessary (corresponding to a priming volume of 580 ml). Requirement for this scale-up is the above described transfer of the fabrication chain to an automated fabrication.

The general, linear scalability of the EGED was shown by comparing the gas transfer of evaluation models consisting of 7 and of 21 layers. The number of necessary layers could be significantly decreased by increasing the number of parallel microchannels in one layer of the blood compartment. The number of necessary microchannels could be decreased by an increased blood flow velocity. Investigations showed that by a blood flow velocity increase from 21 to 35 mm/s (equivalent to a blood flow rate of 8.3 ml/min per layer of the blood compartment) the gas transfer per layer of the blood compartment is increased from 0.3 to 0.4 ml/min for oxygen and from 0.35 to 0.4 ml/min for carbon dioxide. Therefore, the amount of necessary blood compartment layers incorporating 40 parallel microchannels could be decreased to 625. However, it needs to be considered that the increased blood flow velocity would influence the gas partial pressure and oxygen saturation in the outflowing blood negatively. In the experiments a carbon dioxide partial pressure of 37 mmHg and an oxygen saturation of 95.5 % are achieved with an increased blood flow velocity of 35 mm/s. Furthermore, the gas transfer, especially for carbon dioxide, could be increased by reducing the diffusion membrane thickness. A reduced diffusion membrane thickness of 40 μm would allow for a reduction of the blood compartment length to 125 mm without affecting the oxygen and carbon dioxide transfer. This would result in a lower priming volume. In most of the clinical cases a complete supplement of the lung is not necessary. Therefore, devices with fewer layers could be realized for the most common lung support applications. The fine adjustment of the gas exchange could then be performed by adapting the blood flow velocity. Especially in applications with neonates, which accounted for 75 % of the registered extracorporeal respiratory support cases (Paden et al. 2013), a fraction of the above mentioned oxygenation and carbon dioxide removal rates are sufficient. Therefore, EGEDs with 82 layers of the blood compartment cover the physiological gas exchange demand of a neonate considering a bodyweight of 3.5 kg. (Oczenski 2012; Hillier

et al. 2004) The priming volume of such an EGED (57 ml) is in the range of state-of-the-art devices for neonate applications.

Acknowledgments The authors gratefully acknowledge the fruitful collaboration with Novalung GmbH, Heilbronn, Germany and their support by performing the gas exchange characterization experiments

Compliance with ethical standards This study has been supported by Arbeitsgemeinschaft industrieller Forschungsvereinigungen "Otto von Guericke" e.V. (AiFKF2162012FO0). The funders had no role in study design, data collection and analysis, decision to publish, or preparation of the manuscript.

References

O.K. Baskurt, *Handbook of hemorheology and hemodynamics* (Ios Press, Amsterdam, 2007)

J. Brandrup, E.H. Immergut, E.A. Grulke, *Polymer handbook*, 4th edn. (Wiley, New York, 2004)

J.D. Bronzino, *The biomedical engineering handbook*. The electrical engineering handbook series, 2nd edn. (CRC Press, Boca Raton, 2000)

P.M. Bungay, H.K. Lonsdale, M.N. Pinho de. Synthetic membranes. Science, engineering and applications. NATO ASI series. Series C, Mathematical and physical sciences, v. 181. D. Reidel, Dordrecht, (1986)

K.A. Burgess, H. Hu, W.R. Wagner, W.J. Federspiel, Biomed Microdevices (2009). doi:10.1007/s10544-008-9215-2

C.G. Caro, T.J. Pedley, R. Schroter, W. Seed, *The mechanics of the circulation. Oxford medical publications* (Oxford University Press, Oxford, 1978)

Charmilles Technologies. Technologieanleitung Robofil 2020SI, 4929 790 /D/ 10.1997, (1997)

M.E. Cove, G. MacLaren, W.J. Federspiel, J.A. Kellum, Crit Care (2012). doi:10.1186/cc11356

R.C. Eberhart, S.K. Dengle, R.M. Curtis, Artif Organs (1978). doi:10.1111/j.1525-1594.1978.tb00999.x

ELSO Extracorporeal Life Support Organization (2015) ECLS Registry Report. International Summary, January 2015. http://www.elso.org/Registry/Statistics/InternationalSummary.aspx. Accessed 12 January 2015

G.W. Harris, F.C. Tompkins, R.P. deFilippi, J.H. Porter, M.J. Buckley, Development of capillary membrane blood oxygenators, in *Blood oxygenation*, ed. by D. Hershey (Springer US, Boston, 1970), pp. 334–354

S.C. Hillier, G. Krishna, E. Brasoveanu, Neonatal anesthesia. Semin Pediatr Surg **13**(3), 142–151 (2004). doi:10.1053/j.sempedsurg.2004.04.002

D. Hoganson, J. Anderson, E. Weinberg, E. Swart, B. Orrick, J. Borenstein, J. Vacanti, J Thorac Cardiovasc Surg (2010). doi:10.1016/j.jtcvs.2010.02.062

C.T. Kelley, *Solving nonlinear equations with Newton's method* (Society for Industrial and Applied Mathematics, Philadelphia, 2003)

T. Kniazeva, J.C. Hsiao, J.L. Charest, J.T. Borenstein, Biomed Microdevices (2011). doi:10.1007/s10544-010-9495-1

T. Kniazeva, A.A. Epshteyn, J.C. Hsiao, E.S. Kim, V.B. Kolachalama, J.L. Charest, J.T. Borenstein, Lab Chip (2012). doi:10.1039/C2LC21156D

J. Lee, M.C. Kung, H.H. Kung, L.F. Mockros, Microchannel technologies for artificial lungs: (3) open rectangular channels. ASAIO J **54**(4), 390–395 (2008a). doi:10.1097/MAT.0b013e31817eda02

J.K. Lee, H.H. Kung, L.F. Mockros, Microchannel technologies for artificial lungs: (1) theory. ASAIO J **54**(4), 372–382 (2008b). doi:10.1097/MAT.0b013e31817ed9e1

Maquet Cardiopulmonary AG. QUADROX-i Adult und Small Adult Brochure, (2012)

J. Mazumdar, *Biofluid mechanics* (World Scientific, Singapore, 1992)

Medos Medizintechnik AG. MEDOS Hilite 7000 LT Brochure. Oxygenator for Long-term Application, DE-003_2012_11, (2007)

Medtronic Inc. Affinity NT Oxygenation System Brochure, (2011)

Novalung GmbH. iLA Membranventilator. Handbuch für den klinischen Einsatz, DE-2009-01, (2009)

M.L. Paden, S.A. Conrad, P.T. Rycus, R.R. Thiagarajan, ASAIO J (2013). doi:10.1097/MAT.0b013e3182904a52

J.A. Potkay, M. Magnetta, A. Vinson, B. Cmolik, Lab Chip (2011). doi:10.1039/c1lc20020h

R. Margaria. Clin Chem. (11):745–762 (1963)

T. Rieper, C. Mueller, B. Wehrstein, A.N. Maurer, H. Reinecke. in Proceedings of The Sixteenth International Conference on Miniaturized Systems for Chemistry and Life Sciences (μTAS 2012). p. 1801, (2012)

T. Rieper, P. Čvančara, S. Gast, B. Wehrstein, A.N. Maurer, C. Mueller, H. Reinecke. in Proceedings of The Sixteenth International Conference on Miniaturized Systems for Chemistry and Life Sciences (μTAS 2013). p. 1188, (2013)

T. Rieper, P. Čvančara, C. Müller, H. Reinecke, Microfluid Nanofluid (2014). doi:10.1007/s10404-014-1389-8

N. Rochow, A. Manan, W. Wu, G. Fusch, S. Monkman, J. Leung, E. Chan, D. Nagpal, D. Predescu, J. Brash, P.R. Selvaganapathy, C. Fusch, Artif Organs (2014). doi:10.1111/aor.12269

D.H. Schultz, V.L. Shah, W. Shay, P. Wang, Med Biol Eng Comput (1977). doi:10.1007/BF02442952

R. Sillen, E. Swinkels, F. KleinSoetebier, M. Oostveen, J. Huinck, H. Bouwes, N. Bargman. in: Proceedings of the 5th Symposium on Microsystems in Practice, (2004)

R. Skalak, N. Ozkaya, T.C. Skalak, Annu Rev Fluid Mech (1989). doi:10.1146/annurev.fl.21.010189.001123

W. Oczenski. Atmen—Atemhilfen. Atemphysiologie und Beatmungstechnik, 9., überarb. und erw. Aufl. Thieme, Stuttgart, New York, NY, (2012)

W. Wu, N. Rochow, E. Chan, A. Manan, G. Fusch, Lab Chip (2013). doi:10.1039/c3lc41417e